5-2022

Evaluation of Swinging Performance: Quantifying a Surgical Mallet Device

Benjamin M. Schintgen
Western Michigan University Homer Stryker M.D. School of Medicine

Abstract

One of the steps of performing a total hip arthroplasty (THA) is to broach a femoral implant down the femoral canal to add stability down the length of the femur. Broaching consists of surgeons impacting the femoral implant multiple times down the trabecular bone of the femur in increasing size until the implant is sized to either within 3mm of fill of the bone cavity or within surgeon discretion. Fracture of the bone can be caused if the force of impact is too great. Furthermore, surgeons do not know how much force they generate when using an impaction device, such as a mallet. The aim of this study is to build a tool capable of quantifying surgeon mallet swinging performance. G-forces were taken with respect to time from an accelerometer and a Raspberry Pi attached to an orthopedic mallet. Calculations using the g-force were then conducted to identify the velocity of surgeon mallet swing. The importance of velocity calculations in determining the energy available to do work imparted from the surgeon mallet swing is described. Results indicate the device is unable to accurately calculate velocity and thus it requires further development. Ideas for improvement are discussed and potential clinically relevant experiments are proposed for the next device iteration.

Evaluation of Swinging Performance: Quantifying a Surgical Mallet Device

by

Benjamin M. Schintgen

A thesis submitted to Western Michigan University Homer Stryker MD School of Medicine
in partial fulfillment of the requirements for the degree of Master of Science
Medical Engineering
Western Michigan University Homer Stryker MD School of Medicine
May 2022

Masters Committee:

Peter Gustafson, Ph.D., Chair
Steve Butt, Ph.D.,
Keith Kenter, M.D.

Acknowledgements

I would like to thank everyone on my thesis committee, my colleagues in the Medical Engineering program and the greater medical engineering staff for guidance and support throughout the duration of my time in the Master's program. Dr. Peter Gustafson for being my thesis chair and support in device design as well as his mentorship in my career. Dr. Keith Kenter for medical world navigation help and introduction into the orthopedic field. Dr. Steve Butt for aid in College of Engineering resources as well as support in career and thesis. Allin Karhl for 3D printing of simulated bones used as a steppingstone in this study. Dr. Tycho Fredericks for mentorship as an individual. All your guidance throughout this process has been very helpful and fundamental to my education.

I sincerely thank my classmates Avery Waldron, Lilly Ruell, and Brian Ricks for their friendship and support throughout this program. I would not have made it without you.

Finally, I would like to thank my friends and family. Special consideration goes to Merrick Rumel for teaching me basics in Python and C++ coding. Without which, I would not have been able to code a device for this study. I am extremely grateful for all the love and motivation that everyone has shown me especially in the hardest of times. I am eternally grateful.

Table of Contents

Acknowledgements 1

I. Introduction 4

II. Review of Relevant Literature 5

Physics 5

Clinical Need 9

III. Rationale and Objectives 10

Objectives 10

IV. Methods and Procedures 11

Mallet Design 11

Electronics Attachment 14

Center of Gravity Analysis 15

V. Results 17

Center of Gravity Experimentation 17

Coding 19

Charpy Experimentation 22

VI. Discussion 28

Coding 28

Electronics Attachment 29

VII. Limitations 30

Future Studies Recommendation 32

VIII. Conclusions 33

IRB Determination 34

Appendices 36

Appendix 1 Python Code [19] 36

Appendix 2: Datasheet for PCB 352B01 [18] 38
Appendix 3 Clinical Experimentation Description 38
Simulated Bone Design 41
Appendix 3.1 Data Output Model 44
Appendix 3.2 Statistical Analysis of Simulated Post-Processed Data 45
References 48

I. Introduction

Hip osteoarthritis is the most common joint disorder, and is represented by a degenerative process, resulting in pain and functional impairment [1]. According to the Agency for Healthcare Research and Quality, more than 450,000 total hip replacements are performed each year in the United States. Hip replacement surgery is a safe and effective procedure that can relieve pain, increase motion, and facilitate a return to daily activities. Hip replacement surgery is one of the most successful operations in all of medicine [2].

Total Hip Arthroplasty (THA) consists of 4 major components: (i) The damaged femoral head is removed and replaced with a metal stem that is placed into the medullary canal of the femur. The femoral stem may be either cemented or "press fit" into the bone. (ii) A metal or ceramic ball is placed on the upper part of the stem. This ball replaces the damaged femoral head that was removed. (iii) The damaged cartilage surface of the socket (acetabulum) is removed and replaced with a metal socket. Screws or cement are sometimes used to hold the socket in place. (iv) A plastic, ceramic, or metal spacer is inserted between the new ball and the socket to allow for a smooth gliding surface [2]. The part of the procedure that is of focus for this study is the femoral side.

The femoral side of the procedure entails the surgeon starting progressively broaching and removing trial stems that increase in size until the space in the femur is large enough to safely place the correct size femoral stem. This process is done by means of the surgeon swinging a surgical mallet onto the broach to push through bone. However, currently there are no devices that can test bone quality intra-operationally or over smaller bone area and rather is currently measured by DEXA scans that are performed prior to a procedure [3]. Intraoperative bone quality is measured by a two-finger push test that has no repeatability from surgeon to surgeon. Due to this, there is currently no way for surgeons to quantify how they should be striking the bone. Even new technologies used in orthopedic surgeries do not have the ability to aid in any part of the operation on the femoral side other than suggest a stem implant size based on the generated 3D rendering of the femur [4].

Tsiridis et al reported that at the time of THA femoral fractures occur between 5% and 7% post-operation and around .7% during procedure. Implant fractures occur at the time of THA around 2.3% post-operation and .5% during procedure [5]. Intra-operative fractures are mainly due to poor stem sizing or is iatrogenic during impaction of stem [1]. With that, low survivorship on stem (loosening/wearing), is also an issue that occurs 5%-15% within 10 years and 15%-30% within 20 years if the surgeon does not "fill" the femoral canal [1]. As a result, there is also inadequate stem sizing in which subsidence > 3 mm will fail 43.5 times more and stems with varus angulation $\geq 5°$ 12.5 times more [6]. Therefore, it is important to find this balance between fill of the stem in the femoral canal versus iatrogenic fracture.

II. Review of Relevant Literature

Physics

Based off Newtonian physics, the velocity at which a surgeon impacts bone determines the energy the surgeon uses to swing the mallet. That energy is conserved and is directly correlated to the amount of energy that the mallet has on impact of a femoral stem. Furthermore, any object that possesses mechanical energy, can produce work. This means, that the mechanical energy which the surgeon is applying to swing the mallet, enables the mallet to apply a force to the femoral stem. The respective equations describing how energy and force relate to work will be described in more detail.

The number of impactions is important to the study because it is dependent on the bone density and the total amount of work done to progress the stem. Assuming theoretically identical bone densities, the total amount of work done to progress a specific size stem down the femoral canal could be consistent from surgeon to surgeon. However, since no two femurs are similar, it is not currently possible to quantify an independent case of the total amount of work necessary to progress the broach.

Nevertheless, work is defined as the application of a force over a displacement or $W=F\cdot\Delta x$. Where W is total work (J), F total force (N) and Δx is total displacement of the stem (m). If the length of the stem is consistent, the total progression/displacement will be the same from surgeon

to surgeon. This is assuming a consistent definition of placement of being true, a rigid leg, and an identical bone/leg. Understanding this, one can identify the summation of each of the discrete forces applied, multiplied by each discrete change in progression will give the total work. However, each surgeon can be applying a different force in each impact of the stem, causing discrete differences in the progression from impact to impact. A reduction in force application and therefore progression, identifies that there will need to be an increase in discrete applications of work or a larger number of impactions. If the broach handle that the surgeon is using is not directly in line with the broach tip, the component of the discrete axial force is what produces work for progression.

Also, a change in energy is directly proportional to work. This is because the total mechanical energy applied, is equal to the total work. This can be identified by:

$$W = \Delta K + \Delta U + \Delta Erot + \Delta Eth.$$

Where the right-hand side of the equation contains the kinetic energy, potential energy, rotational kinetic energy, and thermal energy respectively. For this study, the thermal energy the surgeon produces in swinging the mallet will not be identified.

The rotational kinetic energy is of key consideration in this work equation as there is a momentum consideration of the arm, hand, and mallet as the system rotates through space and when the mallet strikes the plane. The assumption can be made that the mallet swing is pivoted from the elbow of the surgeon and the wrist remains in the same position for the swing. This means there is a moment about the elbow that can be described by the equation:

$$M_{Elbow} + \sum_{i=1}^{n} \vec{r}_i \times \overrightarrow{F_i} = \alpha I + \vec{r}_g \times (m * a_g)$$

The left-hand side of the above equation is the moment and the forces crossed with their respective moment arms. The right-hand side is change in rotary inertia about the elbow and requires the rotation moments of inertia about that point.

When the arm, hand, mallet connection is in the vertical position, there are no forces producing a moment on the connection. This means that the above equation can be reduced to:

$$M_{Elbow} = \alpha(I_{Arm_{Elbow}} + I_{Hand_{Elbow}} + I_{Mallet_{Elbow}})$$

Where:

$$I_{Arm_{Elbow}} = d_{Arm}^2 m_{Arm}$$

and

$$I_{Hand_{Elbow}} = (L_{Arm} + d_{hand})^2 m_{Hand} + I_{hand}$$

and

$$I_{Mallet_{Elbow}} = (L_{Arm} + L_{hand} + d_{mallet})^2 m_{mallet} + I_{mallet}$$

In the right-hand side of the equations, L represents the length of the respective component, d is the distance from the center of mass to the component end and m is the mass of the component. The I value is the moment of inertia about the respective center of mass.

When the system is at an angle relative to the vertical, there is a force producing a moment that is represented by a component of gravity. When the mallet is not vertical, the moment can better be described by:

$$M_{Elbow} = gcos(\theta)[d_{Arm}m_{Arm} + (L_{Arm} + d_{Hand})m_{Hand} + (L_{Arm} + L_{Hand} + d_{mallet})m_{mallet}] + \alpha(I_{Arm_{Elbow}} + I_{Hand_{Elbow}} + I_{Mallet_{Elbow}})$$

The respective moments of inertia can be substituted back into the component of rotational kinetic energy to describe the work done from a swing. In which the work equation would be expanded from the previously defined equation to be:

$$W = \left(\frac{1}{2}m{v_1}^2 + mgh_1 + \frac{1}{2}I{\omega_1}^2\right) - \left(\frac{1}{2}m{v_2}^2 + mgh_2 + \frac{1}{2}I{\omega_2}^2\right)$$

Assuming a constant change in angular rotation, the velocity (v) will be the same as the angular velocity (ω) at a given point in the rotation. The height (h) is representative of the vertical distance of the center of mass from the top of the swing to the strike. The mass (m) would be the total mass of the arm, hand, and mallet system.

The velocity component in the energy equation has been identified as being of key interest in this investigation. This is because velocity is relevant to the power required to swing the mallet, where power is a measurement of energy transferred per unit time or $P = \frac{dW}{dt}$. Where for a variable force, work can also be defined as $W = \int_{\Delta t} F * vdt$. Using an accelerometer, velocity can be identified from the given accelerations since velocity is the integral of acceleration with respect to time. To be able to calculate the velocity at the point of impact use the equation:

$$\Delta v = \Sigma_{i=1}^{n} dv_i = \Sigma_{i=1}^{n} a_i(dt_i)$$

where i=1 is representative of the point in time of the start of the motion of the mallet and i=n is the point of impact. As can be identified by this equation, identifying the point in time when the mallet starts moving in the direction towards the impact is significant.

In a clinical setting, the mallet will not be at a rest before it is swung for an impact. Rather, the mallet will continuously change direction in a back-and-forth motion, representative of a backwards swing and a striking swing. The swing of importance to this study is the striking swing. The point in time where the swing changes from a backwards swing can be defined as t_0. At time t_0 the initial velocity v_0 should be zero. If the summation of the accelerations and time included values before time t_0, this would present error in the value of a final velocity v_f. Also, at time t_0, the mallet will have an initial position d_0 where $d_f - d_0$ is the distance from the striking plane. The value of $d_f - d_0$ will be different for each swing. Assuming a constant angular velocity, this means that final time t_f will be different. If t_f were to remain constant, v_f would be variable.

For further investigation, an impulse is defined as an integral of force over a time interval or $J(t) = \int_{t1}^{t2} F\ dt$. The impulse from striking the broach handle could have also provided insight to the impact itself because an impulse can described a change in momentum and the forces applied. Where the accelerations provided by the accelerometer could have been integrated over the duration of the short impact. The main utility of the identifying the impulse is that it would be the most direct measure of the energy transferred during impact. Indicating the amount of energy used in broaching and lost during the swing. The investigation to the study of an impulse was an experiment objective not met in this study and should be included in the experiment discussed in *Appendix 3 Clinical Experimentation Description*.

Clinical Need

What constitutes a fracture in an intraoperative setting is a break of the cortical bone from the applied load of the swing causing local stresses. Surgeons impact at an angle relative the transverse direction of the femoral bone based on the different broach handles designs. Broach design effects the energy transmission due to out-of-line impactions and thus gave insight on characterization of impactions necessary to perform a THA with different broach handles [7]. This identifies that the material mechanical properties of cortical bone in both the longitudinal and transverse direction are of key significance to understanding the velocity and the energy that must be available to produce work.

The material properties of bone that are most relevant to fracture in the cortical bone are fracture toughness, modulus and strength. However, porosity and tissue composition, which is a direct result of density, account for more than 75% of the strength and fracture toughness of the cortical bone [8]. As mentioned previously, while there are methods to measure bone porosity and density during THA, their effectiveness is limited due to the subjective description of the surgeon. This means that there is currently no scientifically objective way of determining an accurate amount of energy needed to broach. While this is true, there is still a need for the surgeon to be able to establish control in the energy used to broach.

III. Rationale and Objectives

Having an intra-operative device that measures surgeon mallet velocities can quantify their mallet swinging performance. This study presents an opportunity for a device to be used as a teaching tool with the potential to also be used in a clinical setting for data collection analysis. It is hypothesized that by quantifying their performance, a better repeatability and reproducibility can be established in the surgeon's process. From this, it is speculated that instruction and analysis with this tool may lead to a reduction in the occurrence of fractures and increase the chance of survivorship of the femoral stem. This hypothesizes that there is a potential for improvement of reproducibility in surgeon broach impacts based on the ability to accurately measure the velocity of the mallet swings and the surgeon awareness of these velocities. There is opportunity for further investigation to determine how closely impactions should inter and intra-personally agree in a clinical setting. A description of a possible clinical study will be discussed in *Appendix 3 Clinical Experimentation Description.*

Objectives

The goal of this work is to develop a mallet that can quantify surgeon's performance of mallet impactions by calculating velocity and average number of impactions during femoral stem implantation. This mallet was intended to be used for data acquisition as a teaching tool to provide biofeedback to the surgeon and for potential in clinical data collection analysis. For this reason, the materials needed to be either capable of sterilization or disposable.

The following were the key performance parameters of device design.

1. Calculate velocity of mallet swing as accurately as possible.
2. Maintain location of the CG of mallet with electronic attachments to be as close as possible to the CG of the raw mallet.
3. Make ability for main electronics to be removed from mallet under a minute.

The evaluation to the accuracy of the velocity calculations will be carried out using a Charpy impact tester as later described in the section labelled **Charpy Experimentation.** Where the use

of the Charpy impact tester will be modified to attach the electronics. The location of the CG of the pendulum arm when loaded at a specific height presents relatively simple theoretical calculation of the mallet at the bottom the circular path. This way repeatability of the drop point presents more consistency in a comparative analysis to the raw data collected by the accelerometer.

The location of the CG of the mallet with the attached electronics will be evaluated through measurements of the component's location on the mallet and mathematical calculation. This will be validated with a simple experiment involving suspending the mallet in space by a rubber band. Identifying the CG of the raw mallet will be done with the aid of computer aided drafting 3D modelling software. As well, the ability of the surgeon to remove the main electronics from the mallet for disposal within 5 seconds without it falling off will briefly be discussed.

IV. Methods and Procedures

Mallet Design

To meet the parameters, a design capable of being attached to the mallet and measuring the velocity of the strikes is of key analysis for this study. The first part of investigation into the design is identifying what electronics can perform the intended function. The electronics and their attachment to the mallet can be seen in *Figures 1* & 2 where a detachable, disposable device used to measure velocity is mounted to a surgical mallet.

Figure 1: Mallet design view 1

Figure 2: Mallet design view 2

The device consists of a Raspberry Pi Zero W (www.raspberrypi.com) attached to the MPU-6050 accelerometer (www.invensense.tdk..com), reading g-forces, powered by a rechargeable 5V battery pack. The Raspberry Pi zero W is only $10 according to the Raspberry Pi website. It was chosen as the CPU for this study due to its intuitive OS, the 1GHz single core processor and the 512 MB of RAM available, making it possible for the device to store hundreds of thousands of pieces of raw data [9]. The MPU60 an inexpensive accelerometer sold for $7 a unit [10] Connections between the Raspberry Pi and the MPU6050 were achieved using the I2C interface. The pins that were connected on the accelerometer and Raspberry Pi were the SDA (serial data

line) and SCL (serial data clock) to be able to apply a timestamp to the data collection. MPU6050 delivers raw data through the I2C interface to the memory of a 16GB SD card on the Raspberry Pi.

The MPU6050 contains both a gyroscope and an accelerometer. The gyroscope full scale range of the angular rate sensors are +/-250, +/- 500, +/- 1000 and +/- 2000 °/sec. For the respective scale factors, the sensitivities are 131, 65.5, 32.8, and 16.4 LSB/°/sec with a sensitivity scale factor tolerance of +/-3 and a cross sensitivity factor of +/-2%. [11] Where LSB defines the least significant bit, or the bit furthest to the right in a binary number and cross sensitivity is when one of the axes of the gyro respond to rotation or acceleration in another axis. Also, the output data rate of gyroscope is 8kHz. For a mallet swing, it is anticipated that the range of the angular rate sensor will not need to exceed +/- 500 °/sec. This will be discussed further in the section labelled **Charpy Experimentation**.

The accelerometer is a triple axis accelerometer with 6 degrees of freedom. It has a full-scale ranges of +/-2, +/- 4, +/- 8 and +/- 16g's. The sensitivity scale factor for the accelerometer for the respective ranges are 16384, 8192, 4096, 2048 LSB/g. The cross sensitivity for the accelerometer is also +/- 2%. The maximum output data rate of the accelerometer is 1000Hz [11]. The coordinate system in the gyroscope can be seen on the breakout board in *Figure 3.* The anticipated limits needed for these values will be identified in the **Discussion.**

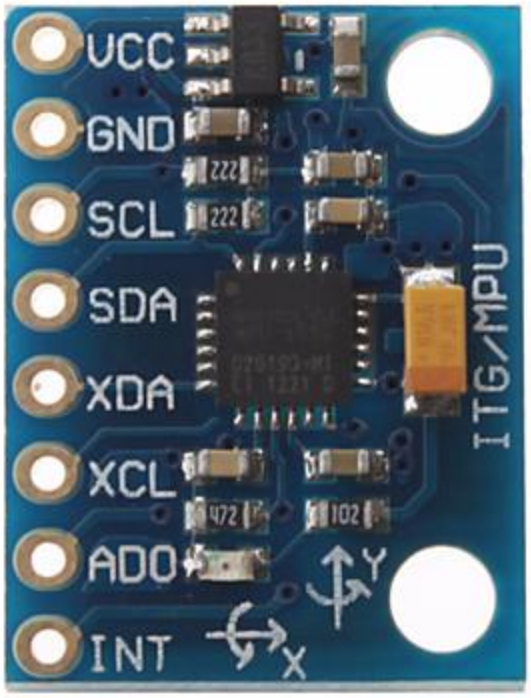

Figure 3: MPU6050 Breakout board [11]

The code seen in *Appendix 1 Python Code* identifies that the raw data which is stored in the memory of the microSD card will not be written in real time as to aid in the speed of data collection. Rather once the data is collected, Raspberry Pi writes the data to a single .csv file in the microSD card. The .csv file is an Excel compatible document, where the data can be transferred for ease of future post-processing.

Electronics Attachment

The methods used for the attachment of the electronics to the mallet, was done by cardboard. The circumference and length of the head of the mallet was measured to be 5.5 inches and 2.5 inches respectively. A single piece of cardboard was cut with the length and width of the dimensions of the mallet head. The cardboard was then rolled to form the shape of a circle. A notch was then placed in the cardboard to accommodate for a slip fit around the head and neck of the mallet. This can be seen in *Figure 4.*

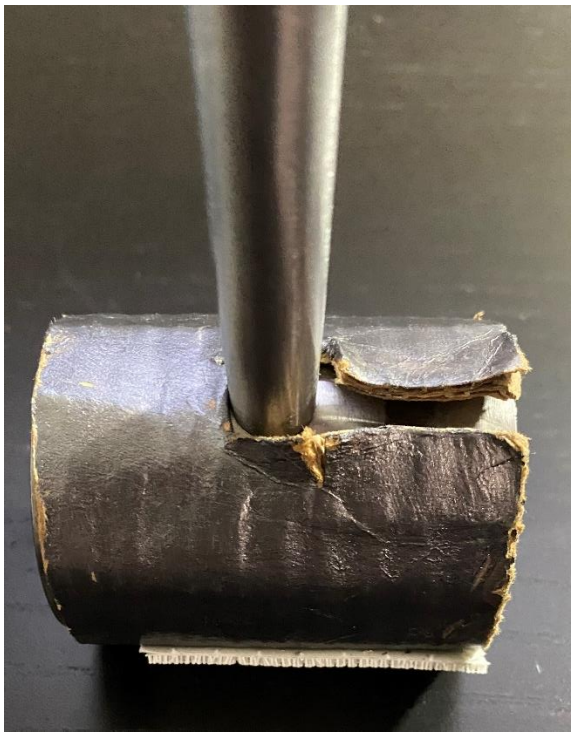

Figure 4: Slide fit mallet attachment

Center of Gravity Analysis

Designing the device so that the CG of the mallet maintains within 5% accuracy was done with the aid of computer aided drafting. The mallet used for this study is a 32oz stainless steel orthopaedic mallet. An assumption was made that the mallet is solid throughout. While the manufacturer has not made a direct claim of this, analysis using computer aided drafting concludes that the mallet was designed so that the CG of the overall device rests close to the axis of the handle to prevent rotation. This can be seen in *Figure 5*, where the CG of the mallet is located 8.94 inches from the bottom of the handle, -0.0046 inches in the y-axis and .0975in in the z-axis. The inertial calculations are reported relative to the CG of the mallet. The handle itself is only 9 inches long, indicating the CG is just before the mallet head.

The battery pack attached to the mallet handle is shrink sleeved along the side of the shaft. The battery pack is 60g/2.11oz with dimensions according to *Table 1*. The CG of the battery pack was placed 6.5 inches from the bottom of the mallet. Wiring and layout of the MPU6050

accelerometer and Raspberry Pi were placed in such a way to balance the CG of those components over the axis of the handle. The weights of the MPU6050, the Raspberry Pi and the attachment are 2.1g/.07oz, 9g/.31oz, and 3g/.1oz respectively. The electronics were attached 9.875in from the bottom of the mallet and the attachment was concentric around the mallet head. This height the electronics were placed was chosen so that the accelerometer would be in a quadrant where the z-axis would be parallel to the Earth. This is to hopefully not read any vectors due to gravity in more than 2 axes as the mallet is vertical.

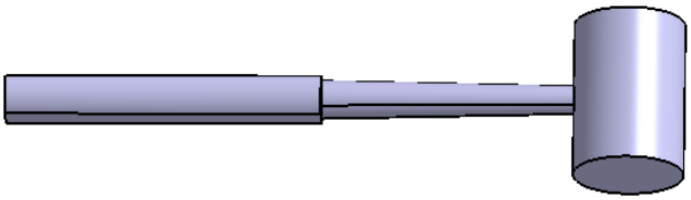

Characteristics		Center of Gravity (G)	
Volume (in^3)	9.19266	Gx (in)	8.949
Area (in^2)	38.44357	Gy (in)	-0.0046
Mass (lb)	2.02	Gz (in)	0.09755
Density (lb/in^3)	0.22		

Inertia Matrix/G			
IoxG (lb*in^2)	0.9873	IxyG (lb*in^2)	0
IoyG (lb*in^2)	21.74	IxzG (lb*in^2)	0
IozG (lb*in^2)	22.172	IyzG (lb*in^2)	-0.0206

Figure 5: Computer aided drafting: center of gravity analysis of standard mallet design

Battery Dimensions	
Length (mm)	95 ± .2
Width (mm)	26.5 ± .2
Height (mm)	22 ± .2

Table 1: Rechargeable battery dimensions [12]

By following calculations for CG along the axis of the handle indicates the new location of the CG to be:

mal_oz = 32;
mal_CG = 8.94;
elect_oz = .31+.07+.1;
elect_CG = 9.875;
bat_oz = 2.11;
bat_CG = 6;
New_CG =
((mal_oz*mal_CG)+(elect_oz*elect_CG)+(bat_oz*bat_CG))/(mal_oz+elect_oz+bat_oz);

Where the new CG is located a distance of 8.15 inches from the bottom of the handle along the axis of the handle. This identifies a change in CG of 8.4% in this direction. However, there is a moment that occurs due to the battery pack not being inline with the handle axis. The CG is located 11mm/.433in from the handle axis. This means that the battery creates a moment of .25 N*m and shifts the CG in the respective direction .026 inches towards the battery.

The calculations done for the inertias as shown in *Figure 5* are about the CG of the mallet itself. Since the location of the CG of mallet/electronics system moved further away from the accelerometer, the inertia at the point of the accelerometer will be larger from the axis of rotational and this will increase the increase the angular momentum at the accelerometer. However, for ease of calculation, assumptions can be made that the distance of the accelerometer away from the center of gravity is insignificant relative to the mass of the system.

V. Results

Center of Gravity Experimentation

A simple experiment was conducted to test the actual location of the center of gravity of the mallet. For this experiment, a rubber band was placed around the handle of the mallet and repositioned in such a way so the mallet would suspend freely without tipping to one side or the other. The location of the CG of the raw mallet can be seen in *Figure 6. Figure 6* identifies that

the CG of the raw mallet was at 8inches from the bottom of the handle. This means the assumptions in the calculations done in the methods, about the entirety of the mallet being solid was not accurate.

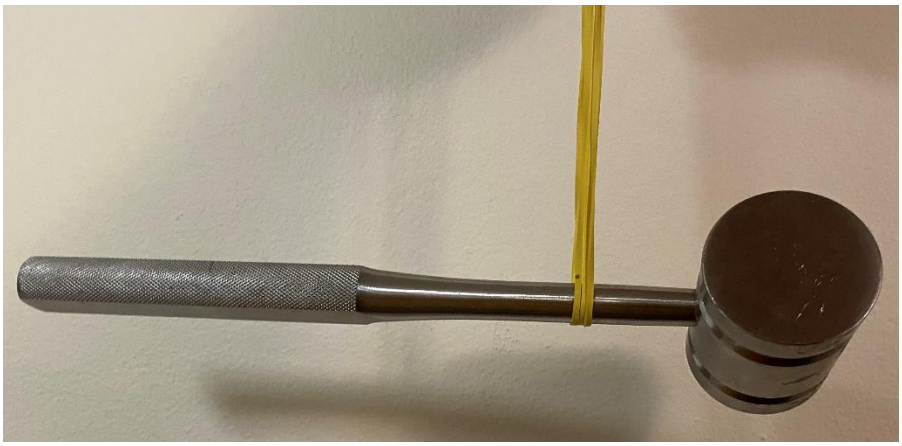

Figure 6: True location of CG of raw mallet

When the electronics were attached to the mallet in the previously described configuration, the CG of the mallet was found to be 8.0625 inches from the bottom of the handle. This can be seen in *Figure 7.* The actual CG of the mallet had only moved .0625inches and created a .78% change along the length of the mallet. The difference between the actual CG of the mallet with the electronics and the theoretical CG of the mallet with the electronics is a 1.07% error.

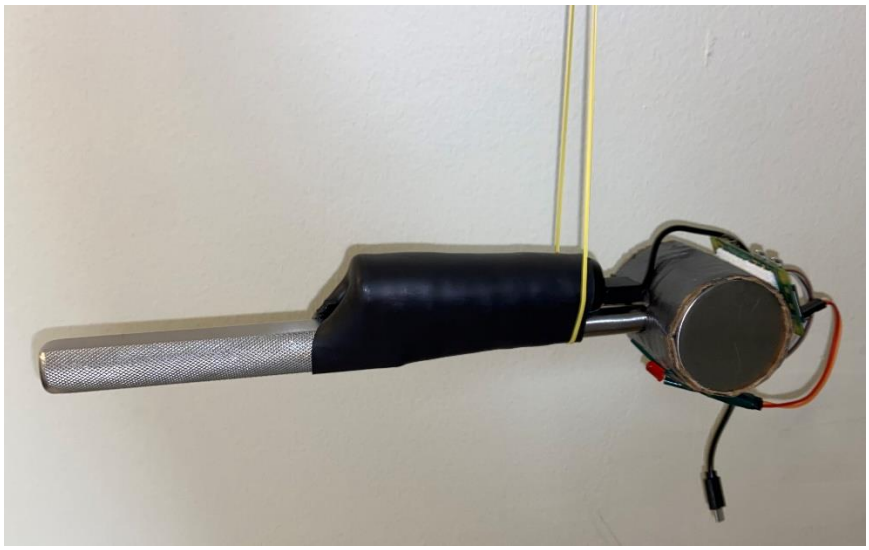

Figure 7: True location of CG of mallet with electronics

Coding

The first half of the code present in *Appendix 1 Python Code* up until the python program calls out def main():, is a way for the Raspberry Pi to identify that it is interacting with the MPU6050. The main function starts with addressing that the respective I2C interaction with the MPU6050 is occurring with the respective raspberry Pi pins. The data is written and stored in a .csv file labeled "output" with data representing a timestamp and the X, Y and Z accelerations in different data columns.

In the velocity calculations there is a measured gravity vector as the accelerometer's coordinate system rotates about its 6 degrees of freedom. These gravity vectors describe accelerations in a local coordinate system. This can be seen in *Figure 8*. In *Figure 8*, the -Y cardinal direction of the accelerometer starts by facing towards the Earth at rest. The accelerometer reads a value of +1g in the Y direction to signify that the accelerometer is opposing the acceleration due to gravity in the y direction. The accelerometer is then rotated to that the +X axis indication of the accelerometer is facing the Earth. At this point, the acceleration in the y direction dropped to 0g's and the acceleration in the X direction dropped to -1g's. This is without any linear movement in either direction while just representing rotation.

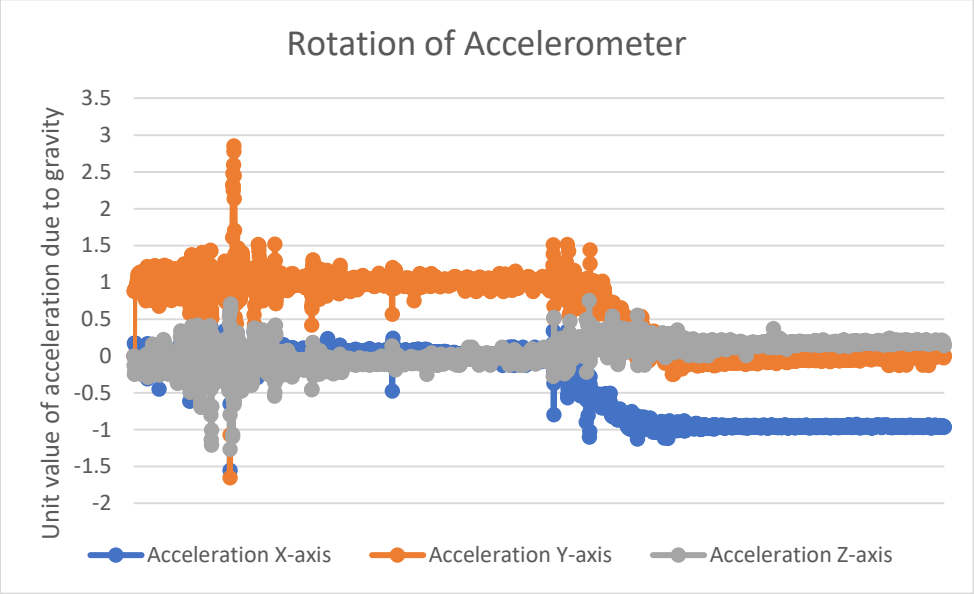

Figure 8: Example of changes in g-force without change in velocity

The best velocity calculations can be seen of a freefall from a 1m height. *Figure 9*, expresses 2 examples of a freefall from a 1m height in the -Y orientation. Upon closer investigation, zooming into the sampled data set, one can see that the acceleration oscillates at a value of +1g before making a rapid decline down to 0gs until the mallet hits the floor and has a rapid spike to indicate the event. This can be seen in *Figure 10*.

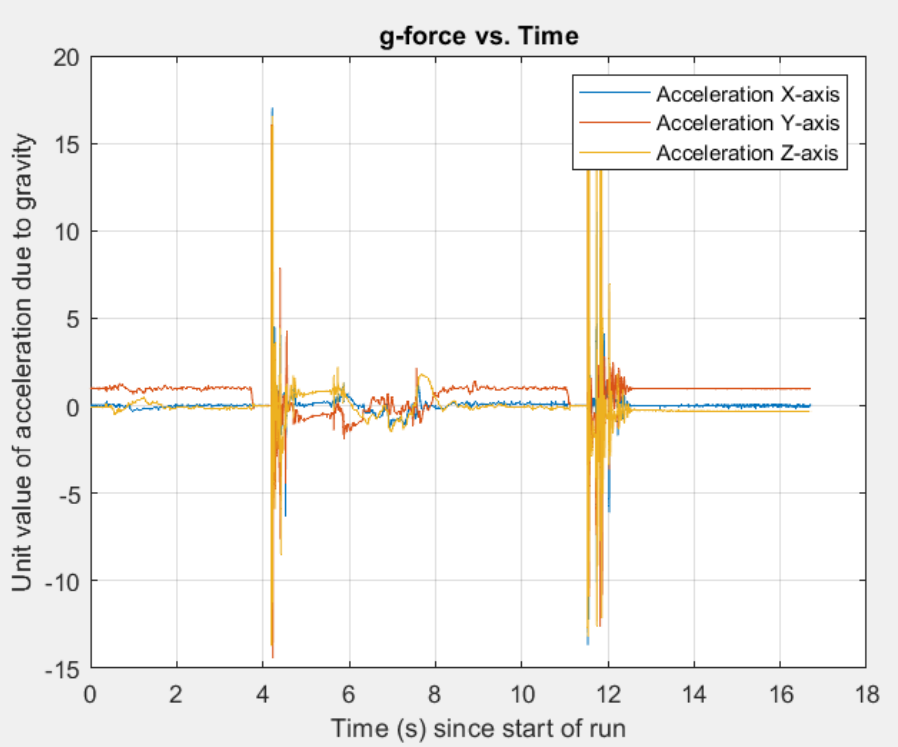

Figure 9: Graph of Acceleration vs Time of 2 drops from a 1m height

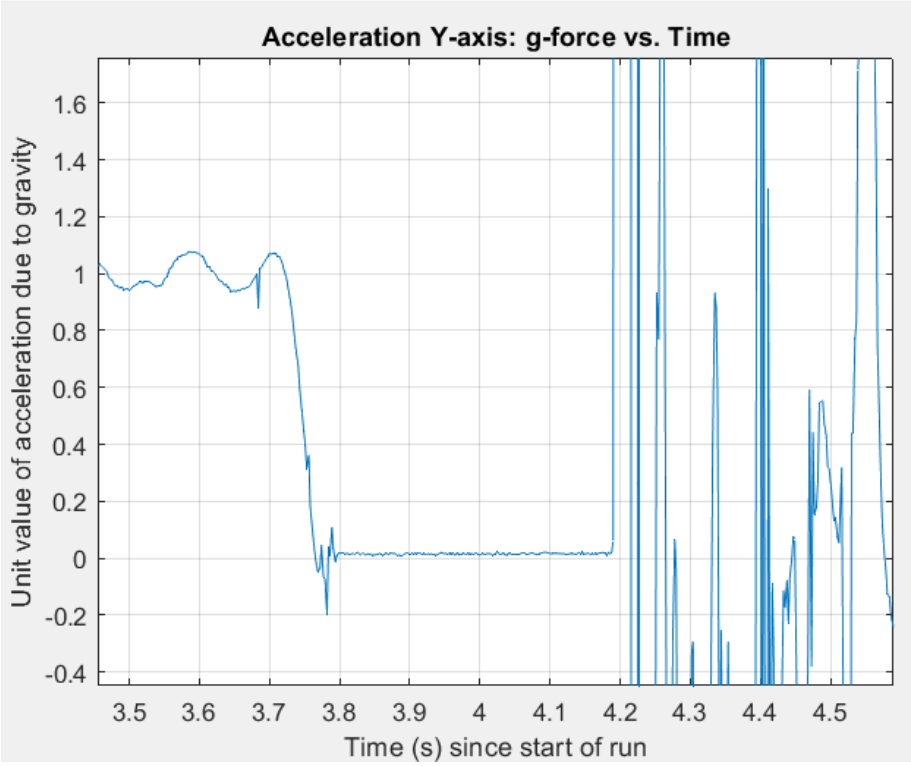

Figure 10: Indication of acceleration due to gravity for 1m drop.

Newtonian physics identify that when an object is dropped from a height of 1m from initially at rest, the velocity the object will have will be 4.429 m/s and the time to fall will be .4515s. 2D linear motion also identifies that the final velocity up until impaction is directly proportional to the gravity vector based on the accelerometer orientation. This can be seen in the 2D equations where at any time velocity can be represented by:

$$v_{f_x} = t * gcos(\theta)$$
$$v_{f_y} = t * gsin(\theta)$$

Where the y axis is pointed towards the earth and the x-axis is pointed left of the observer. Since theta is 90 degrees for a 1m drop, the final velocity in the y, based off the equation could be just gravity multiplied by time. Using the example of an object dropped from a 1 m height, the velocity was calculated by multiplying gravity by time. This is because with the local coordinate system, the accelerations being outputted were zero. Meaning that calculation could not be done by means of a summation of discrete accelerations multiplied by the discrete changes in time.

The velocity recorded in this calculation came to be 4.3123m/s. This identifies a 2.6% error in the actual velocity calculation. This analysis can be seen in F*igure 11* as shown in the figure on the left where the velocity curve peaks at 4.3123m/s.

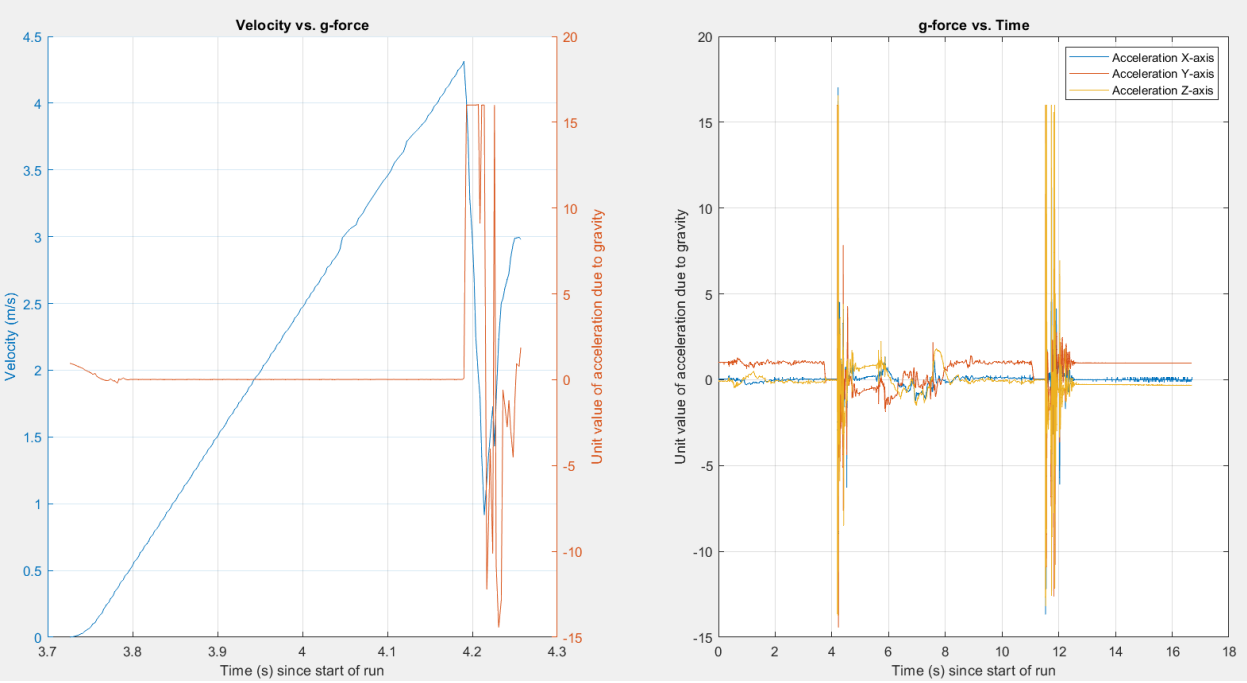

Figure 11: Velocity analysis of 1m drop.

Charpy Experimentation

An experiment using a Charpy impact tester was conducted to validate the capability of the device to measure the velocity as it moves through a circular path. A Charpy impact tester is typically used as a standardized high strain-rate test to determine the amount of energy absorbed by a material during a fracture [13]. At the point of an impact with the Charpy tester, there is a known amount of kinetic energy. The impact energy is based off to which the striker has risen. This energy can be used to determine the velocity of the striker at the point of impact when it was released from the predetermined height. Attaching the accelerometer at the same distance away from the pivot point as the striker should lead to calculations of velocity with similar values.

For this study, the electronics were mounted on the main mass at the bottom of the tester by means of electrical tape as can be seen in *Figure 12*. The accelerometer was mounted at the same distance away from the pendulum pivot point as the impactor. It was assumed that the location of the impactor is the CG of the pendulum arm. When the pendulum arm was elevated, the device was 6.37° above parallel at the low setting of the latch. This placed the new vertical height of the CG of the pendulum, and the location of the accelerometer, at a height of 1m above their respective locations at the bottom of the swing. This can be seen in *Figure 13*. The accelerometer was oriented so that the +x direction was facing towards the Earth at the bottom of the swing and the -y direction faced the left of the device from the view in *Figure 12*.

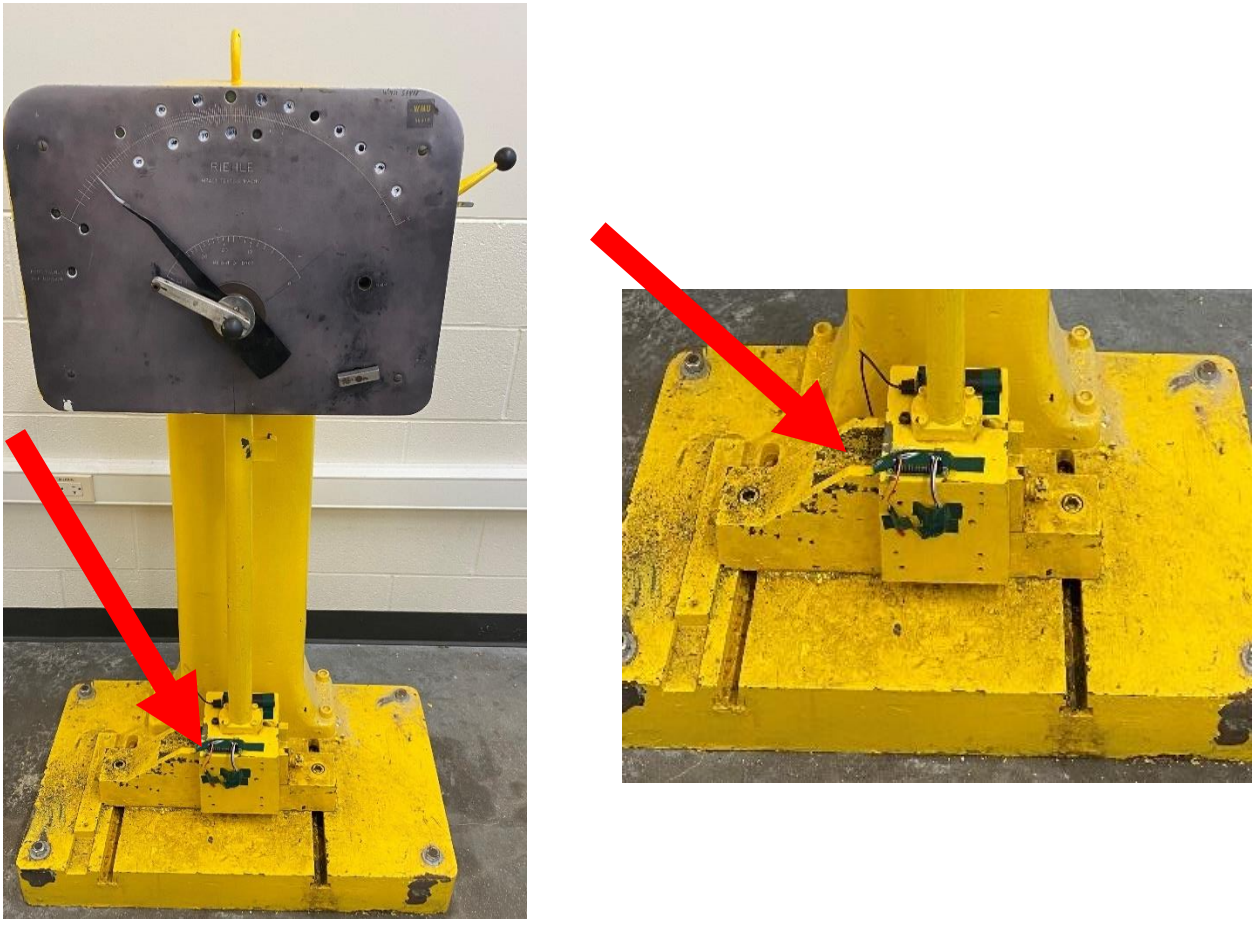

Figure 12: Charpy Impact Tester with electronics attached via green electrical tape.

Figure 13: Charpy Impact Tester at low setting

Through conservation of energy, the potential energy that is present from the device at rest from the position in *Figure 13* will be transferred to kinetic energy at the bottom of the swing. This is assuming negligible friction from the device and negligible air resistance. This means that:

$$\Delta KE = \Delta PE$$

$$\frac{1}{2}mv^2 = mgh$$

$$v = \sqrt{2gh}$$

At a height of 1m, the tangential velocity of the accelerometer should be 4.429m/s. If the velocity is solved for with rotational kinetic energy, the equations can be described by:

$$\Delta KE_{rot} = \Delta PE$$

$$\frac{1}{2}I\omega^2 = mgh \qquad \text{where} \qquad I = ml^2$$

$$mgh = \frac{1}{2}ml^2\omega^2$$

$$\omega = \sqrt{\frac{2g}{l^2}}$$

$$v = \sqrt{\frac{2g}{l^2}} * l$$

Where the height is still 1m and the length (l) from the pivot point is .9m, the velocity also comes to 4.429m/s at the bottom.

The pendulum design of this test should indicate velocities in the x and y axes that are like the exponential decay of a device in simple harmonic motion. The resulting accelerations from this motion can be found in *Figure 14.*

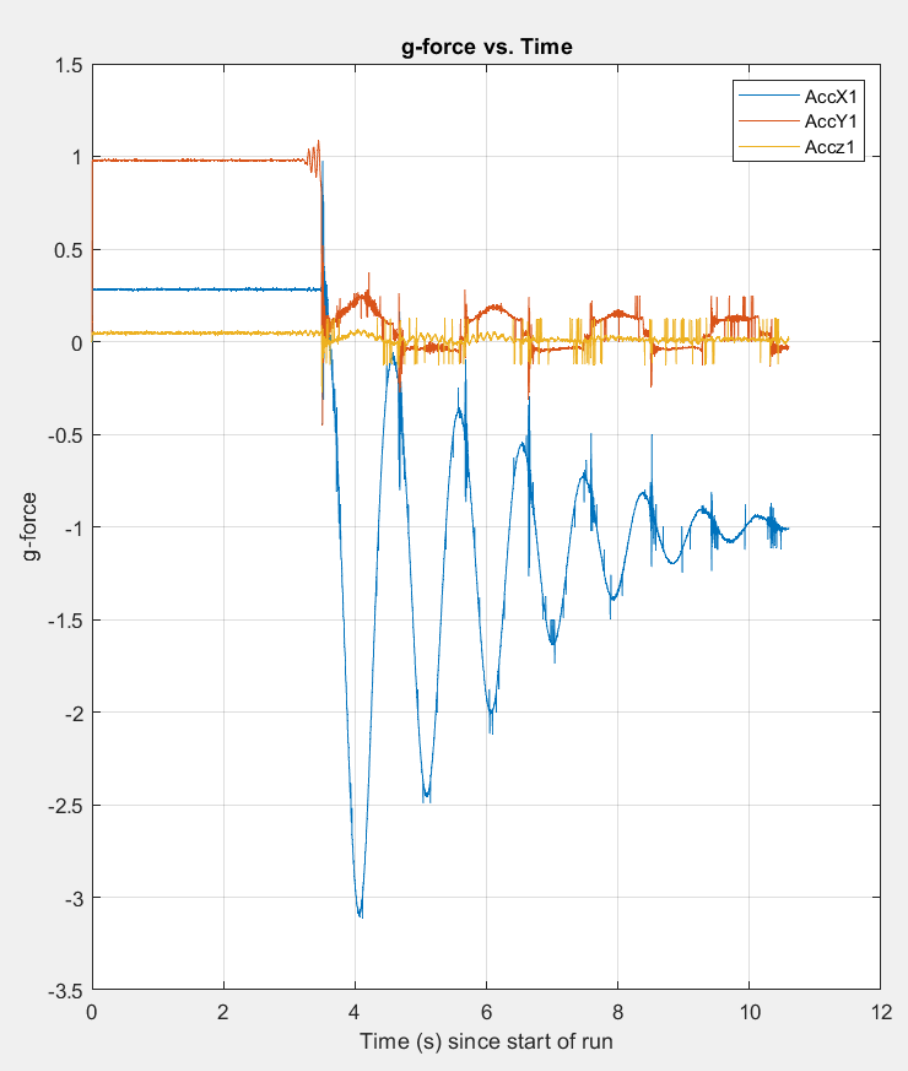

Figure 14: Results of accelerations in Charpy Test.

The graphical representation of the accelerations present in *Figure 14* are based off a local coordinate system. In a local coordinate system, when the accelerometer is stationary with an axis at or close to normal with the Earth, the acceleration should be a unit value of 1g. In this coordinate system, the acceleration in the direction of Earth (in this case the +x-axis) should immediately drop to 0 at a point of release, non-zero between the horizontal and vertical, and then zero again when the axis is parallel to the Earth. However, the y-axis acceleration should also have an oscillating characteristic as it passes through the bottom of the swing as well. Rather it indicates several peaks accelerations in the same direction.

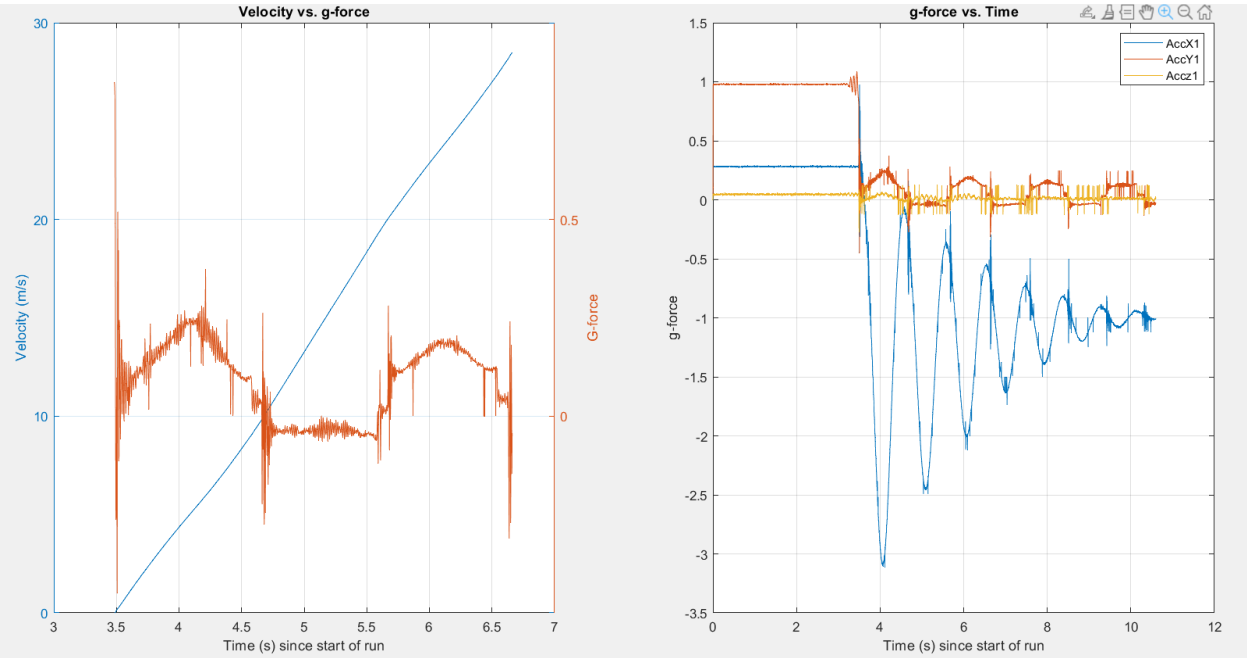

Figure 15: Analysis of velocity in the

As can be seen in *Figure 15*, velocity is on a linearly upward trend exceeding 20m/s within that duration. This may indicate that without tracking in an inertial reference frame, the accelerometer gives readings in a local frame that operate under the assumption that gravity only acts in 1 axis. The axis of rotation for the device is about the z-axes. As the accelerometer rotates about the z-axis, both the x and y axes should be reading components of gravity relative to the axis's angle to the Earth. Transformation of measured accelerations into an inertial reference frame would allow calculation of a velocity vector and their contributions to energy. Making it so that the accelerometer outputs accelerations at a constant value of zero under rotation.

The range of the angular rate sensor for this application did not need to exceed +/-250°/sec. This was because the change in angle from the release point to the bottom was 96.37° and took .4515 seconds to occur. This means the angular rate did not exceed 213.44°/sec. However, if inaccuracy in the gyroscopic angles of rotation occurs due to drift a significant error in the velocity can occur in multiple axes. Further investigation should be done to establish the amount of drift present. The cross sensitivity brought about in the assembly of the board also identifies that there may be some error in accurately calculating the inertial reference frame acceleration.

This is because the rotation has a slight error in correcting for the orientation of the accelerometer when the gravity vector is present.

VI. Discussion

Coding

According to Preutenborbeck et al., typical mean mallet velocities are measured between 5m/s and 5.5m/s [7]. Preutenborbeck et al. identifies that broach progression varies between 2mm and .5mm and the broach progression decays exponentially with each impact [7]. The equation for determining the average g-force of an object in freefall in a shock situation is (h/d)*g0 where h is the height of the object, d is the distance traveled during an impact and g0 is representative of the acceleration due to gravity at +1g. Assuming that the accelerometer were falling towards the earth from a plane perpendicular to the earth a distance 1m away. The upper limit of g-force that the impact will undergo will be somewhere between 500gs and 2000gs given the distance of broach progression. These values can be classified as an upper limit because the leg and the table will absorb an unknown fraction of motion.

The literature identifies that the time duration of the event is on the order of magnitude of 2ms for the entire decay with the event occurring in a duration of .1ms [14] This identifies that the order of magnitude of data collection should be on the order of 10kHz or larger. While the Raspberry Pi has a clock rate of 1GHz, the Pi under I2C only has the capacity in high-speed mode to transfer data at 3.4Mbps. 4 16 bits of information is being read by the device. Meaning that a theoretical limit for the Raspberry Pi to collect data from the I2C configuration is at a frequency of 53.125kHz [15]. Python is an interpretive language which causes some overhead as the Raspberry Pi must interpret the language as opposed to potentially coding is C++ or a language made directly for the device such as Arduino language with Arduino.

According to the spec sheet of the accelerometer, the best possible data rate that could be transferred through I2C is 4597Hz, but the programmable range of the output data rate has a max of 1000Hz [11]. While the theoretical output rate should be 1KHz, the raw data that is collected was only appears to be at 450Hz. It is worth noting that there also seems to be a caching buffer.

Meaning that when transmission of the raw data falls behind the ability to receive, the accelerometer put the data in a cache for future transmission. The accelerometer also has a limit of reading +/-16g's which is well under the limit of identifying the event, but not entirely necessary for conducting velocity calculations. The 450hz data collection rate suggests that the entire duration of the event was missed. The spike in the data is representative of either noise or the bounce from the impaction. For the continuation of velocity calculations, a full-scale range is not necessary if the frequency has the capability of identifying the duration of the event. This is because the acceleration felt by the mallet as it swings through the air will be no larger than an order of tens of g's.

It is also worth noting, the intended impulse measurement described in *Appendix 3 Clinical Experimentation Description* could still provide accurate data even with the problem of rotating local coordinate systems. This is due to the short duration of the event and the limited change in frame of reference over the duration. It would also be easier to calculate a delta V only over the short duration due to the limited change in reference. However, the available full-scale range and high data collection frequency would not represent the impulse with the current electronics. Also, the accelerometer averages the accelerations over the sampling duration. With a low sampling rate, the accelerations provided would give an approximation to the overall change in momentum. It would be worth investigating in a future study what the error would be in the change of momentum.

Electronics Attachment

From the design of the mallet attachment, one side of the cardboard attachment had a path the neck could travel through. The attachment could potentially slip off under a large enough shock. While there has been no sign of slippage of the attachment during impaction, it would be worth investigating into a latch that would close this opening at a tighter tolerance closer to the neck. The cardboard should also be substituted for a more sterile substitute such as a high-density polyethylene. While the attachment does not come into direct contact with any biomaterial or absorb any of the force from the mallet, it needs to be resistant to shock and be presented as sterile. HDP would be a good substitute because it has a low moisture absorption, can potentially resistant high impacts, and will not retain any biomaterial [16].

VII. Limitations

One of the limitations specific to the velocity calculation is that there is not a distinct point in time when the electronics start to collect a change in acceleration. The analysis makes the user identify a start time t_0 of the motion, for calculations. This can be seen in the 1m drop test. The mallet was held in space so that the y-axis of accelerometer is oriented towards Earth. The accelerometer will pick up vibrations that would be represented graphically as oscillations at the unit value of acceleration. The mallet was held at the CG so that when the mallet was allowed to freefall, it would not cause the axis to change orientation with respect to gravity. The initial velocity $v_0$of the mallet was assumed to be zero as it rested from a height of 1m. Due to this, the time t_0 that was chosen for calculations of velocity was taken from the accelerations a_0 to a_f. The value a_0 began from the point at which the data concluded oscillating and dropped beneath the unit value of +1g down to zero. This can be seen int the MATLAB code:

```
dtime2 = diff(time2)                        %difference in time between 2-
                                            %points of data
r2 = [1499:1700]                            %range of data points selected
v2 = 9.81*(1-AccY2(r2)).*dtime2(r2)         %Velocity for each data point
v2 = cumsum(v2);                            %Cumulative sum of velocity
maxv2 = max(v2);                            %Maximum value of velocity
```

The initial time t_0 and acceleration a_0 were taken from the data point labelled 1499. The final time t_f and final acceleration a_f were at point 1700 indicated by the strike. Velocity was calculated by multiplying the accelerations at each of the data points through that time interval by the difference in time between each data point. In the case of this example, if a value of t_0 was selected after the start of motion (after point 1499), the full change in velocity will not be recorded, as seen in *Figure 16* where the velocity is lower than the 4.3123m/s.

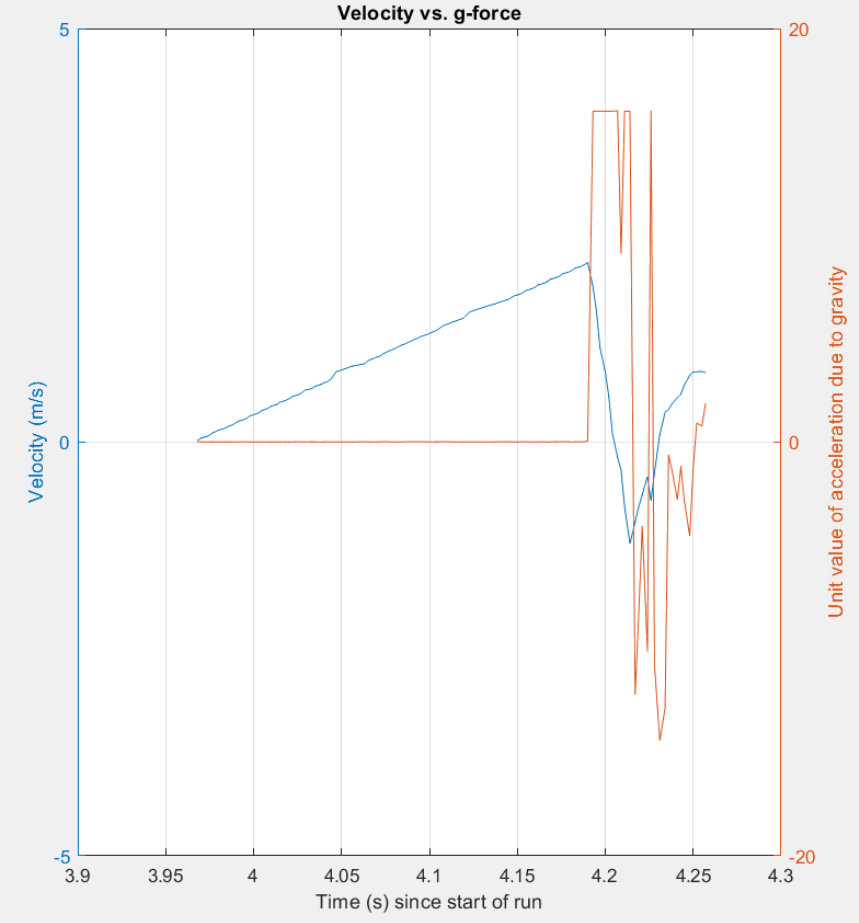

Figure 16: Partial range of velocities over time

What is needed is to transform from the local system to the global system such that the gravity vector can be properly tracked and the inertial reference frame velocity can be calculated. Inertial reference frame acceleration is based off an observer's orientation to the object being measured. This way, the object has a clearer indication of when in motion. Otherwise, calculations are done with respect to the acceleration of the Earth rather than by the person operating the device. The other limitations were due the sampling rate and full-scale range of data sampling. Data sampling should occur at a frequency of about 10+KHz and have a full-scale range of |+/-5000|g's to accurately measure an impact. For the continuation of velocity calculations, a full-scale range is not necessary if the frequency has the capability of identifying the duration of the event. This is because the acceleration felt by the mallet as it swings through the air will be no larger than an order of tens of g's.

Future Studies Recommendation

In a continued study, suggestions for use of different electronics should be done with the use of piezo-electrics. For continuation with a velocity calculation study for an intra-operational device this study would recommend looking for a piezo electric like that of the 830M1-2000 triaxial conditioning monitor. 830M1-200 is manufactured by TE and is classified as a condition monitoring accelerometer specifically for vibration, impact, and shock monitoring. The range of the accelerometer is from +/-2000gs with a 5000g shock limit. It also has a flat frequency response rate 15KHz in all three axes. The 830M1 can sense and measure motion and acceleration in all three orthogonal axes and provides analog voltage outputs that represent the signal magnitude in each axis. However, the accelerometer must be properly oriented during assembly to be level with a respective axis to ensure that it will accurately sense the magnitude of vibration and motion in the proper axes [17]. The respective specifications can be seen in *Appendix 2: Specifications for 830M1-2000* [18]. 830M1-2000 is available for a single unit price of $152 from Mouser [17].

Along with this device, an analog to digital converter as well as a stable power source will be needed because the voltages from the piezo system will need to be converted to readable data. This could be done by attaching a Wheatstone bridge and an amplifier to a PCB that could be directly wired to an Arduino or similar CPU. The weight and size of this device are 1g and 0.6 x 0.06 in. Soldering to a PCB could be an option that would has the potential to lie within dimensional size constraints for the electronics' attachment to the mallet. Further calculations can then be done, given the readings from the accelerometer, to identify the forces without the need of purchasing a specialized force transducer. Further testing involving the device metrics and experimental objectives described in **Appendix 3 Clinical Experimentation Description** would identify whether surgeons would benefit from the aid of a device that could potentially quantify their performance by calculating and identifying their velocities for them.

VIII. Conclusions

This work identified the initial steps in being able to quantify the swings of a surgical mallet device used by a surgeon. An analysis on the capabilities of using a standard wireless CPU and low +/-g range accelerometer was investigated mainly due to its inexpensiveness. Analysis suggests linear velocity calculations can be run to consistency within a 3% error. Manual mallet swings representative of motion in a circular pattern are not capable of being calculated without an accurate inertial reference frame. In a localized reference frame with a gravity vector output, the accelerometer operates under the assumption that gravity only acts in 1 axis. Inertial reference frame was not used as a basis for this study due to the researcher's limited understanding of gyroscopic Euler angles and unit quaternions and how they could be related to the respective axes of acceleration.

Experimentation on the location of the CG was conducted as the electronics were not to add any excess ergonomic burden to the user. CG analysis using the respective electronics and choice of locations moved the location of the actual CG of the mallet .0625inches up the handle. The placement of the battery created a moment of .25N*m that will add a rotational effect to the mallet. As well, the design of a slip fit for the electronic materials allow ease of installation and removal.

Discussion of the conducted experiments provide an understanding of what is further necessary to be able to accurately quantify the swing of a mallet. A continued investigation in evaluating surgeon performance should be conducted as seen in **Appendix 3 Clinical Experimentation Description.** This experimentation will help identify if the aid of such a device is effective in preventing fractures and improving THA outcomes.

IRB Determination

EXEMPT DETERMINATION

March 29, 2022

Peter A Gustafson, PhD
Western Michigan University Homer Stryker M.D. School of Medicine
Department of Medical Engineering
1000 Oakland Drive
Kalamazoo, MI 49008

IRB#: WMed-2021-0818 *(please reference this number in all correspondence with the IRB)*

PROTOCOL TITLE: Comparative analysis of THA force Impaction events with and without an intra-operational force impulse device

Dear Dr. Gustafson:

The above referenced protocol and associated materials were reviewed on 03/28/2022 and it has been determined that it meets the criteria for exempt status as described in 45 CFR Part 46.104 (d) Category 3: Research involving benign behavioral interventions in conjunction with the collection of information from an adult subject through verbal or written responses (including data entry) or audiovisual recording if the subject prospectively agrees to the intervention and information collection and at least one of the following criteria is met: (i)(B) Any disclosure of the human subjects' responses outside the research would not reasonably place the subjects at risk of criminal or civil liability or be damaging to the subjects' financial standing, employability, educational advancement, or reputation.

The IRB reviewed the following documents related to the determination:

- Application for Initial Review Form Submitted 03/20/2022, 03/28/2022
- Study Protocol version - No version date
- Implied Consent Form version 4 dated 03/28/2022
- Data Output Model - No version date
- Thesis Data - No version date
- Data Record Sheet – No version date

Although your research involves human subjects, it is not subject to the regulations requiring IRB continuing review and approval. However, it is important to understand that an exemption from IRB review and approval is not equal to an exemption from the investigator responsibilities and institutional policies governing human subjects research at WMU Homer Stryker M.D. School of Medicine. This information can be accessed on the medical school website.

In order to capitalize on the spirit of exempt research, submit any changes to the IRB only if it no longer meets the criteria for exemption and/or the conditions of the waiver of HIPAA

authorization outlined above. If you are not sure, please contact the IRB office at the contact information below.

Please note changes to your IRB application related to key research personnel must be reported to the IRB via a Personnel Change Form which can be accessed in the electronic system. Keep in mind only individual(s) accessing identifiable data and/or interacting with research subjects should be added. The IRB will acknowledge these addition(s) or removal(s).
If you have any questions, please contact the WMed IRB office at 269-337-4345 or email irb@med.wmich.edu.

Sincerely,

Parker Crutchfield, PhD
IRB Chair
Western Michigan University Homer Stryker M.D. School of Medicine
1000 Oakland Drive
Kalamazoo, MI 49008-8012

cc: Benjamin M Schintgen, Keith Kenter, M.D., Steven Eric Butt, Ph.D.

Appendices

Appendix 1 Python Code [19]

```
import time
import smbus2
import csv
from datetime import datetime, timezone
import RPi.GPIO as GPIO

PWR_MGT_1 = 0x6B
CONFIG = 0x1A
SAMPLE_RATE = 0x19
GYRO_CONFIG = 0x1B
ACCEL_CONFIG = 0x1C
ACCEL_X_HIGH = 0x3B
ACCEL_Y_HIGH = 0x3D
ACCEL_Z_HIGH = 0x3F
GYRO_X_HIGH = 0x43
GYRO_Y_HIGH = 0x45
GYRO_Z_HIGH = 0x47
TEMP_OUT_HIGH = 0x41
MAX_G = 16

def MPU_initialization(bus, Device_Address):
    bus.write_byte_data(Device_Address, PWR_MGT_1, 1)
    bus.write_byte_data(Device_Address, SAMPLE_RATE, 0)
    bus.write_byte_data(Device_Address, CONFIG, 0)
    bus.write_byte_data(Device_Address, GYRO_CONFIG, 24)
    bus.write_byte_data(Device_Address, ACCEL_CONFIG, 0x18)

def Read_data(reg_add, bus, Device_Address):
    high = bus.read_byte_data(Device_Address, reg_add)
    low = bus.read_byte_data(Device_Address, reg_add+1)
    value = (high<<8)|low
    if value>35768:
        value = value-65536
    return value

def main():
    bus = smbus2.SMBus(1)
    Device_Address = 0x68
    MPU_initialization(bus, Device_Address)
    GPIO.setmode(GPIO.BCM)
```

```
    GPIO.setup(26, GPIO.OUT)
    GPIO.output(26, GPIO.LOW)
    with open('output.csv', 'w') as f:
        writer = csv.writer(f)
        header = ['Timestamp', 'Acc X', 'Acc Y', 'Acc Z' ]
        writer.writerow(header)
        while 1:

            ACCEL_X = Read_data(ACCEL_X_HIGH, bus, Device_Address)
            ACCEL_Y = Read_data(ACCEL_Y_HIGH, bus, Device_Address)
            ACCEL_Z = Read_data(ACCEL_Z_HIGH, bus, Device_Address)

            Ax = ACCEL_X/2048.0
            Ay = ACCEL_Y/2048.0
            Az = ACCEL_Z/2048.0

            if Ax >= MAX_G or Ay >= MAX_G or Az >= MAX_G:
                GPIO.output(26, GPIO.HIGH)
            writer.writerow([datetime.now() ,Ax, Ay, Az])



if __name__ == "__main__":
    main()
```

Appendix 2: Datasheet for PCB 352B01 [18]

SPECIFICATIONS

- ±25g to ±2000g dynamic ranges
- 15000Hz bandwidth
- ±1.25V amplified signal output
- $3.3V_{DC}$ to $5.5V_{DC}$ excitation voltage range
- -40°C to +125°C operating and storage temperature range
- 1.5V to 5.5V maximum supply voltage
- 5000g maximum shock limit (any axis)
- -2kV to +2kV maximum ESD
- 200µA average supply current
- 100Ω output impedance
- 1-second warm-up
- 0 to 100% ambient humidity range
- IP68 protection, hermetic package
- 3.3g in weight

Appendix 3 Clinical Experimentation Description

The original aspects of the above study that were not met should take place in the continuation of the study. Clinical trials with residents and attending surgeons should be conducted for analysis of the impulses and the quantity of impactions where both quantities are independently meaningful. An outcome that was not achieved from the above study explored the option of characterizing the impulse or change in momentum of the mallet impact itself. Impulse is defined as the integration of force over a change in time or $J(t) = \int_{t1}^{t2} F\ dt$. Accelerometers, such as the MPU6050 used in the above study, have the capacity to output data of g-forces with a respective timestamp. The g-forces that the accelerometers are collecting are a unit measurement of acceleration which is directly proportional to the force applied by the mallet due to the mallet's constant mass. Due to this, the value of the g-force acceleration is very characteristic of the size of the impulse.

It is speculated that a surgeon delivering the same impulse on a bone with heavy osteoporosis vs a bone that just exhibits osteopenia presents a greater risk of fracture to the bone with heavy osteoporosis. This is a hypothesis that should be tested. The outcome of testing this hypothesis will determine if surgeons should receive feedback on the performance of their swing with respect to the bone density. Since there is currently not a quantitative metric for the impulse required to broach down different bone densities, arbitrary accelerations should be selected as representative of the impulse required to broach down 3 different bone densities. The magnitude of the accelerations found in the impaction event should be directly proportional to the density of the bone (more dense = higher acceleration).

In continuation of device design, the following performance metrics that should be met are:

1. Calculate impulse with <5% error
2. Identify 3 arbitrary acceleration values characteristic of impacting different bone densities and code for LED feedback if the acceleration passed the limit on a given trial.

Once the device performance metrics have been met, an experiment should be conducted with volunteers who possess a range of orthopedic surgical experience. The experiment that should take place in future study should investigate the following:

Outcome 0: Mean impact impulse and average number of impactions should be gathered over a series of experiments.

There are 4 independent hypotheses that should be tested through experimentation with surgeons. The first is that the mean impulse and number of impactions will each be more consistent if the surgeon receives real time feedback. The second is that the mean impulse and number of number of impactions will be more consistent with an increase in surgeon experience. Third, there will be statistically significant differences in surgeon-to-surgeon mean impulse and number of impactions. Fourth, there will be statistically significant differences in mean impulse and number of impacts as a function of bone quality. These hypotheses are in anticipation that consistency in impulse and number of impactions, would correlate with both reductions in intraoperative and postoperative harms to the patients.

The experiment testing these metrics should report the respective characteristics on Data Output model found in *Appendix 3.1 Data Output Model*. To record these values, the experiment should be conducted in the following way:

To keep consistency, the surgeons that should be used to conduct the study will all use the same orthopedic mallet. In this way, the CG of the mallet-device combination can be calculated and will be known to be constant throughout the duration of the study. Data collection with the device will be kept on throughout the experiment and continuously collect data even when the

surgeon does not receive real time feedback. This is to reduce the potential of changing the impaction habits of the surgeons throughout the duration of the test as much as possible.

Data collection will take place in two different stages. Each surgeon will be given an unlimited number of swings/practice attempts to get accustomed to the instrumented mallet before stage 1. The first stage of the study will collect data without surgeon feedback, so the surgeons are less likely to be affected by the measurement. In the second stage, feedback will be presented in numerical, graphical, or some other suitable form. For consistency, the same mallet will be used for both stages of the study. The surgeon will have unlimited opportunity between stages to become accustomed to the feedback mechanism.

For a power analysis, the groups can be subclassified as seen *in Appendix 3.2 Statistical Analysis of Simulated Post-Processed Data.* Where the groups are as followed:

- Mean impulse and number of impactions with feedback vs. without
- Mean impulse and number of impactions of resident with feedback vs. attending with feedback
- Mean impulse and number of impactions resident without feedback vs. Attending with feedback
- Mean impulse and number of impactions comparison between residents
- Mean impulse and number of impactions comparison between attending
- Impulse value per impact

The group that will be the least powered group comparison will involve the surgeons subclassified by experience. Upon assuming a large effect size (f=1.01) [20], a preliminary power analysis suggests that 5 surgeons per group will be necessary. The groups will be A and B where 1 group consists of residents and 1 group consists of attending surgeons. Subsequently, the study will have to consist of an ANOVA analysis. The average and standard deviation of the data will be found to determine whether the data presents adequate information on the performance of the surgeon's mallet impacts. The same analyses should be run on whether surgeon feedback with the presented data from the device affects the number of impactions the surgeon does. This will be a representation of intra-surgeon consistency.

The study will be done with 1 of 5 potential “strikers” and 1 of 3 values coded into the device, representative of different forces that could be used for different bone densities. The experimentation on bone densities is a proof of concept for surgeon mallet impactions. Materials of varying densities can be used as the control to test the surgeons without having identical characteristics to bone. With that, it is assumed that surgeon mallet impact impulses will vary with bone density.

By testing these variables based on the arbitrary acceleration values that will be used to represent bone density, the study should be able to tell how these variables interact. More specifically, each of the potential 5 surgeons will use a total of 3 bone specimens. They can operate on 1 bone specimen with the one “stem”. However, they will need to do so on 3 different sets of bones with varying bone densities representative of the coded value. This will be done both with and without feedback from the device. This will mean that each surgeon will be used to conduct 6 sets of data both with feedback and without feedback. A data collection table can be seen in *Appendix 3.1 Data Output Model*.

Examples with simulated post-processing using Minitab with data representing an analysis to each of the 4 experimental metrics can be shown in *Appendix 3.2 Statistical Analysis of Simulated Post-Processed Data*.

Simulated Bone Design

For the use of conducting the experiment to investigate the 4 experimental metrics, 3 groups of simulated bones were designed, and 3D printed as reference values for 3 different densities as shown in *Figure 17*. The 3D prints were created at 3 distinct fills to indicate the varying bone densities. For this study, 2 different CAD files were combined to make a distinction between the difference of cortical bone and trabecular bone. The cortical bone was printed out of a PLA plastic and is attached in such a way as to be interlocked with the polyurethane trabecular bone so the 2 different materials do not separate from the vibrations or axial forces that they will be undergoing.

Figure 17: Top view of cylindrical bone simulants with 3 different densities

A hollowed cylinder was chosen as the shape of the simulated femur to mimic the shaft of the bone. An aluminum rod is used in place of the cobalt chromium and titanium stems. The subjects used in the proposed future investigation will use the data acquisition mallet to create a press fit between the aluminum rod and the 3D printed bone substitute to mimic surgical broaching. The polyurethane inner wall of the hollowed cylinder has dimensions to fit tightly to the diameter of the aluminum rod. This can be seen in *FIGURE 18*. The infill between the PLA cortical and the polyurethane trabecular inner wall has elasticity varying according to the densities. This means that the press fit of the cylindrical rod into the 3D printed bone should theoretically require less powerful and overall, a smaller number of impacts.

Figure 18: Press fit of aluminum rods into bone surrogate

The printing of the bone surrogates should have dimensions like that of an average femur. The aluminum rods should have a length like that of different size stems. The average length of an adult male femur is 480 mm and the female femur is between 431 and 457 mm [21]. Femoral thickness averages about 23.4mm and the thickness of femoral cortical bone is an average of 3mm. [21],[22] Stem length range from 95mm to 125mm [23] The hollowed space used for the press fit should be printed to the dimensions of the thickness of the desired manufacturers implant. A thickness of the respective surrogate trabecular bone can then be established.

Printing infills for the surrogate bone were 40%, 25% and 15% respectively. These infills were picked as arbitrary values to provide a proof of concept on pressing down a material with different densities.

To quantify a person's bone mineral density, the result of a test such a DEXA scan is compared with the average results of a healthy 25- to 35-year-old of the same sex and ethnicity. The standard deviation between the two is representative of a t-score [3] Each integer difference in a t-score value is representative of a 10% difference in bone density [24]. A drop in the infill percentage of the 3D printed material was used to simulate the feel of bone that exhibits properties of lower t-scores and thus characteristic of having more osteoporosis.

Appendix 3.1 Data Output Model

Data Output Model

Bone Density "1" g/cm^3

		Res 1	Res 2	Res 3	Res 4	Res 5	Att 1	Att 2	Att 3	Att 4	Att 5
without feedback	trial 1										
	trial 2										
with feedback	trial 1										
	trial 2										

Bone Density "2"g/ cm^3

without feedback	trial 1										
	trial 2										
with feedback	trial 1										
	trial 2										

Bone Density "3" g/cm^3

without feedback	trial 1										
	trial 2										
with feedback	trial 1										
	trial 2										

(Res = Resident; Att = Attending)

Each box represents a computer dataset containing information on the following possible parameters:

Impact force
impulse curve vs time
number of impacts
number of impacts over warning indicator
peak impulse value

The following parameters will be recorded on the "Data Record Sheet":

Resident or attending
Years of surgeon experience

Appendix 3.2 Statistical Analysis of Simulated Post-Processed Data

WORKSHEET 1

One-way ANOVA: mean imp w/, mean imp w/o

Method

Null hypothesis	All means are equal
Alternative hypothesis	Not all means are equal
Significance level	α = 0.05

Equal variances were assumed for the analysis.

Factor Information

Factor	Levels	Values
Factor	2	mean imp w/, mean imp w/o

Analysis of Variance

Source	DF	Adj SS	Adj MS	F-Value	P-Value
Factor	1	2.2	2.175	0.08	0.783
Error	498	14249.2	28.613		
Total	499	14251.4			

Model Summary

S	R-sq	R-sq(adj)	R-sq(pred)
5.34910	0.02%	0.00%	0.00%

Means

Factor	N	Mean	StDev	95% CI
mean imp w/	250	6.060	7.184	(5.395, 6.724)
mean imp w/o	250	5.928	2.370	(5.263, 6.592)

Pooled StDev = 5.34910

WORKSHEET 1

One-way ANOVA: resident w/, attending w/

Method

Null hypothesis	All means are equal
Alternative hypothesis	Not all means are equal
Significance level	α = 0.05

Equal variances were assumed for the analysis.

Factor Information

Factor	Levels	Values
Factor	2	resident w/, attending w/

Analysis of Variance

Source	DF	Adj SS	Adj MS	F-Value	P-Value
Factor	1	2.2	2.192	0.04	0.837
Error	248	12848.5	51.808		
Total	249	12850.7			

Model Summary

S	R-sq	R-sq(adj)	R-sq(pred)
7.19781	0.02%	0.00%	0.00%

Means

Factor	N	Mean	StDev	95% CI

resident w/	125	5.966	7.940	(4.698, 7.234)
attending w/	125	6.153	6.370	(4.885, 7.421)

Pooled StDev = 7.19781

WORKSHEET 1

One-way ANOVA: resident w/o, attending w/o

Method

Null hypothesis	All means are equal
Alternative hypothesis	Not all means are equal
Significance level	α = 0.05

Equal variances were assumed for the analysis.

Factor Information

Factor	Levels	Values
Factor	2	resident w/o, attending w/o

Analysis of Variance

Source	DF	Adj SS	Adj MS	F-Value	P-Value
Factor	1	1.87	1.866	0.31	0.578
Error	248	1490.94	6.012		
Total	249	1492.80			

Model Summary

S	R-sq	R-sq(adj)	R-sq(pred)
2.45190	0.13%	0.00%	0.00%

Means

Factor	N	Mean	StDev	95% CI
resident w/o	125	6.048	3.061	(5.616, 6.480)
attending w/o	125	5.875	1.628	(5.443, 6.307)

Pooled StDev = 2.45190

WORKSHEET 1

One-way ANOVA: resident 1, resident 2, resident 3, resident 4, resident 5

Method

Null hypothesis	All means are equal
Alternative hypothesis	Not all means are equal
Significance level	α = 0.05

Equal variances were assumed for the analysis.

Factor Information

Factor	Levels	Values
Factor	5	resident 1, resident 2, resident 3, resident 4, resident 5

Analysis of Variance

Source	DF	Adj SS	Adj MS	F-Value	P-Value
Factor	4	51.31	12.83	0.35	0.843
Error	245	8928.41	36.44		
Total	249	8979.73			

Model Summary

S	R-sq	R-sq(adj)	R-sq(pred)
6.03676	0.57%	0.00%	0.00%

Means

Factor	N	Mean	StDev	95% CI
resident 1	50	5.931	2.708	(4.250, 7.613)
resident 2	50	6.685	2.800	(5.003, 8.366)
resident 3	50	6.323	5.316	(4.641, 8.004)
resident 4	50	5.408	6.938	(3.727, 7.090)
resident 5	50	5.69	9.52	(4.00, 7.37)

Pooled StDev = 6.03676

WORKSHEET 1

One-way ANOVA: attending 1, attending 2, attending 3, attending4, attending 5

Method

Null hypothesis	All means are equal
Alternative hypothesis	Not all means are equal
Significance level	α = 0.05

Equal variances were assumed for the analysis.

Factor Information

Factor	Levels	Values
Factor	5	attending 1, attending 2, attending 3, attending4, attending 5

Analysis of Variance

Source	DF	Adj SS	Adj MS	F-Value	P-Value
Factor	4	41.99	10.50	0.48	0.748
Error	245	5322.98	21.73		
Total	249	5364.97			

Model Summary

S	R-sq	R-sq(adj)	R-sq(pred)
4.66116	0.78%	0.00%	0.00%

Means

Factor	N	Mean	StDev	95% CI
attending 1	50	5.709	1.208	(4.410, 7.007)
attending 2	50	6.347	2.837	(5.048, 7.645)
attending 3	50	5.964	3.612	(4.666, 7.263)
attending4	50	5.463	6.535	(4.164, 6.761)
attending 5	50	6.588	6.586	(5.289, 7.886)

Pooled StDev = 4.66116

WORKSHEET 1

One-way ANOVA: imp 1, imp 2, imp 3, imp 4, imp 5

Method

Null hypothesis	All means are equal
Alternative hypothesis	Not all means are equal
Significance level	α = 0.05

Equal variances were assumed for the analysis.

Factor Information

Factor	Levels	Values
Factor	5	imp 1, imp 2, imp 3, imp 4, imp 5

Analysis of Variance

Source	DF	Adj SS	Adj MS	F-Value	P-Value
Factor	4	611.1	152.78	3.05	0.018
Error	245	12285.5	50.14		
Total	249	12896.6			

Model Summary

S	R-sq	R-sq(adj)	R-sq(pred)
7.08130	4.74%	3.18%	0.81%

Means

Factor	N	Mean	StDev	95% CI
imp 1	50	5.188	7.016	(3.215, 7.160)
imp 2	50	7.80	7.57	(5.83, 9.77)
imp 3	50	5.865	6.171	(3.892, 7.837)
imp 4	50	7.683	6.786	(5.711, 9.656)
imp 5	50	3.66	7.75	(1.69, 5.63)

Pooled StDev = 7.08130

References

[1] Apostu, D., Lucaciu, O., Berce, C., Lucaciu, D., & Cosma, D. (2018). Current methods of preventing aseptic loosening and improving osseointegration of titanium implants in cementless total hip arthroplasty: a review. In Journal of International Medical Research (Vol. 46, Issue 6, pp. 2104–2119). SAGE Publications Ltd. https://doi.org/10.1177/0300060517732697

[2] Total Hip Replacement - OrthoInfo - AAOS. (n.d.). Retrieved July 25, 2021, from https://orthoinfo.aaos.org/en/treatment/total-hip-replacement/

[3] Bone densitometry. Johns Hopkins Medicine. (n.d.). https://www.hopkinsmedicine.org/health/treatment-tests-and-therapies/bone-densitometry.

[4] MAKO THA Surgical Guide. (n.d.).

[5] Tsiridis, E., Haddad, F. S., & Gie, G. A. (2003). The management of periprosthetic femoral fractures around hip replacements. In Int. J. Care Injured (Vol. 34).

[6] Townsend, S., Kim, S. E., & Pozzi, A. (2017). Effect of stem sizing and position on short-term complications with canine press fit cementless total hip arthroplasty. Veterinary Surgery, 46(6), 803–811. https://doi.org/10.1111/vsu.12666

[7] Preutenborbeck, M., Reuter, J., & Ferrari, E. (2020). Quantitative characterisation of impaction events during femoral broaching in total hip arthroplasty. Medical Engineering and Physics, 76, 13–19. https://doi.org/10.1016/j.medengphy.2019.12.004

[8] Morgan, E. F., Unnikrisnan, G. U., & Hussein, A. I. (2018). Bone Mechanical Properties in Healthy and Diseased States. *Annual Review of Biomedical Engineering*, *20*, 119. https://doi.org/10.1146/ANNUREV-BIOENG-062117-121139

[9] Raspberry Pi Zero W - DEV-14277 - SparkFun Electronics. (n.d.). Retrieved August 8, 2021, from https://www.sparkfun.com/products/14277

[10] *MPU6050 Gy521 cheap 6DOF IMU (Accelerometer & Gyro) imus*. https://www.jsumo.com/. (n.d.). Retrieved May 7, 2022, from https://www.jsumo.com/mpu6050-gy521-cheap-6dof-imu-accelerometer-gyro

[11] MPU-6000 and MPU-6050 Product Specification Revision 3.4 MPU-6000/MPU-6050 Product Specification. (2013).

[12] Xu, J., & Shen, ---Tristan. (2019). Specification Approval Sheet Name: Power Bank Model: 51126 SPEC: 2500mAh (Black body, support 20mA output) Approved By Checkup Make. www.Tenergy.com

[13] Saba, N., Jawaid, M., & Sultan, M. T. H. (2019). An overview of mechanical and physical testing of composite materials. *Mechanical and Physical Testing of Biocomposites, Fibre-Reinforced Composites and Hybrid Composites*, 1–12. https://doi.org/10.1016/B978-0-08-102292-4.00001-1

[14] Crisman, A., Yoder, N., Mccuskey, M., Meneghini, M., & Cornwell, P. (n.d.). Femoral Component Insertion Monitoring Using Human Cadaveric Specimens.

[15] I2C quick guide - analog devices. (n.d.). Retrieved May 2, 2022, from https://www.analog.com/media/en/technical-documentation/product-selector-card/i2cb.pdf

[16] *Choosing the Best Plastic for Medical Equipment*. (n.d.). Retrieved May 6, 2022, from https://www.piedmontplastics.com/blog/best-plastics-for-medical-equipment

[17] 830M1 triaxial condition monitoring accelerometer - mouser.com. (n.d.). Retrieved May 5, 2022, from https://www.mouser.com/datasheet/2/418/7/ENG_DS_830M1_Triaxial_Accelerometer_A1-2090513.pdf

[18] *830M1 Triaxial Condition Monitoring Accelerometers - TE Connectivity / Measurement Specialties | Mouser*. (n.d.). Retrieved May 3, 2022, from https://www.mouser.com/new/te-connectivity/te-connectivity-830m1/

[19] *MPU6050 (Accelerometer+Gyroscope) Interfacing with Raspberry Pi |...* (n.d.). Retrieved May 15, 2022, from https://www.electronicwings.com/raspberry-pi/mpu6050-accelerometergyroscope-interfacing-with-raspberry-pi

[20] Lakens, D. (2013). Calculating and reporting effect sizes to facilitate cumulative science: a practical primer for t-tests and ANOVAs. Frontiers in Psychology, 0(NOV), 863. https://doi.org/10.3389/FPSYG.2013.00863

[21] *Difference Between Male and Female Femur | Compare the Difference Between Similar Terms*. (n.d.). Retrieved May 16, 2022, from https://www.differencebetween.com/difference-between-male-and-female-femur/

[22] Treece, G. M., Gee, A. H., Mayhew, P. M., & Poole, K. E. S. (2010). High resolution cortical bone thickness measurement from clinical CT data. *Medical Image Analysis*, *14*(3), 276. https://doi.org/10.1016/J.MEDIA.2010.01.003

[23] Feyen, H., & Shimmin, A. J. (2014). Is the length of the femoral component important in primary total hip replacement? *Bone and Joint Journal*, *96 B*(4), 442–448. https://doi.org/10.1302/0301-620X.96B4.33036/ASSET/IMAGES/LARGE/33036-GALLEYFIG2.JPEG

[24] Borchardt, G., Nickel, B., Andersen, L., Hetzel, S., Illgen, R., & Hennessy, D. et al. (2022). Femur and Tibia BMD Measurement in Elective Total Knee Arthroplasty Candidates. Journal Of Clinical Densitometry. https://doi.org/10.1016/j.jocd.2022.01.004